Published in final edited form as:
Adv Funct Mater. 2010 December 8; 20(23): 4196–4205. doi:10.1002/adfm.201000932.

The Contribution of DOPA to Substrate–Peptide Adhesion and Internal Cohesion of Mussel-Inspired Synthetic Peptide Films

Travers H. Anderson,
Department of Chemical Engineering, University of California, Santa Barbara, CA 93106, USA

Jing Yu,
Department of Chemical Engineering, University of California, Santa Barbara, CA 93106, USA

Abril Estrada,
Department of Molecular Cell & Developmental Biology, University of California, Santa Barbara, CA 93106, USA

Dr. Malte U. Hammer,
Department of Chemical Engineering, University of California, Santa Barbara, CA 93106, USA

Prof. J. Herbert Waite, and
Department of Molecular Cell & Developmental Biology, University of California, Santa Barbara, CA 93106, USA

Prof. Jacob N. Israelachvili*
Department of Chemical Engineering, University of California, Santa Barbara, CA 93106, USA

Abstract

Mussels use a variety of 3, 4-dihydroxyphenyl-L-alanine (DOPA) rich proteins specifically tailored to adhering to wet surfaces. Synthetic polypeptide analogues of adhesive mussel foot proteins (specifically mfp-3) are used to study the role of DOPA in adhesion. The mussel-inspired peptide is a random copolymer of DOPA and N^5 -(2-hydroxyethyl)-L-glutamine synthesized with DOPA concentrations of 0–27 mol% and molecular weights of 5.9–7.1 kDa. Thin films (3–5 nm thick) of the mussel-inspired peptide are used in the surface forces apparatus (SFA) to measure the force–distance profiles and adhesion and cohesion energies of the films in an acetate buffer. The adhesion energies of the mussel-inspired peptide films to mica and TiO_2 surfaces increase with DOPA concentration. The adhesion energy to mica is 0.09 μJ m^{-2} $mol_{DOPA}{}^{-1}$ and does not depend on contact time or load. The adhesion energy to TiO_2 is 0.29 μJ m^{-2} $mol_{DOPA}{}^{-1}$ for short contact times and increases to 0.51 μJ m^{-2} $mol_{DOPA}{}^{-1}$ for contact times >60 min in a way suggestive of a phase transition within the film. Oxidation of DOPA to the quinone form, either by addition of periodate or by increasing the pH, increases the thickness and reduces the cohesion of the films. Adding thiol containing polymers between the oxidized films recovers some of the cohesion strength. Comparison of the mussel-inspired peptide films to previous studies on mfp-3 thin films show that the strong adhesion and cohesion in mfp-3 films can be attributed to DOPA groups favorably oriented within or at the interface of these films.

* jacob@engineering.ucsb.edu .

Supporting Information
Supporting Information is available from the Wiley Online Library or from the author.

1. Introduction

Marine animals such as mussels have mastered the art of wet adhesion. Adhering to wet surfaces poses a number of problems including the existence of a water boundary layer on the wet surfaces which inhibits molecular contact between the adhesive and the substrate. The ability of the mussel to overcome these obstacles has inspired much research in an attempt to understand the mechanism of mussel adhesion[1-3] as well as to develop biomimetic adhesives for underwater and medical applications.[4-6] Mussel adhesion is mediated by the byssus which consists of a bundle of threads, each attached to the mussel at one end and to a substrate at the opposite end by a flattened plaque. Currently, eight proteins have been identified and characterized from the plaques of which mussel foot proteins (mfps) 3, 5 and 6 are found at the plaque-substrate interface and appear to be most responsible for the ability of the mussel to adhere to wet surfaces.[7,8] One distinguishing characteristic of all the mfps is the presence of the post-translational modification of tyrosine to 3,4-dihydroxyphenyl-L-alanine (DOPA). Although DOPA is found throughout the byssus it is present in higher amounts in the mfps found at the plaque-substrate interface and can be as high as 30 mol% in mfp-5.[9] DOPA is obviously an important component in wet adhesion but its contribution is not yet well understood.

Until recently, almost all that was known about the chemical reactivity of DOPA concerned its reactivity in solution, particularly its redox activity.[10,11] There are many examples in literature of catechols and hydroquinones being involved in nucleophilic and free radical reactions, however only two have been observed in peptidyl-DOPA; i) 5- and 2-S-cysteinylDOPA crosslinks are common in green mussel (*Perna*) byssus[12] and the plaque footprints of blue mussels (*Mytilus)*[8] and ii) 5, 5′-diDOPA crosslinking is distributed throughout the byssus and reaches 1 mol% in the plaque.[13]

The coordination chemistry of DOPA has also been studied extensively. Mfp-1 as well as its consensus deca-peptide sequences were shown to form stable bis- and tris-catecholate complexes with Fe III at pH 7.5 in vitro[14,15] as well as in *Mytilus* byssus.[16] Monahan & Wilker[17] also showed that the addition of Fe^{3+} to acid extracted foot proteins significantly improves their cohesive strength. Additionally, catechol has been shown to form bidentate binuclear surface structures with TiO_2 surfaces.[18] DOPA-metal coordination with metal oxide surfaces has also been seen with polymer-tethered DOPA on oxides of Ti IV and Fe III.[19,20] The strength of the DOPA-TiO_2 coordination bond has recently been under scrutiny as two papers have reported AFM measurements of the bond strength of single DOPA residues interacting with a TiO_2 surface in aqueous conditions that differ by an order of magnitude.[19,21]

The adhesion mechanisms of mfp-1 and -3 thin films have also been studied in the surface forces apparatus.[22] Although both mussel proteins have similar DOPA content, pI and backbone flexibility, mfp-3 was observed to bridge two mica surfaces together whereas mfp-1 merely coated the mica surfaces and only bridged the two surfaces after significant mechanical stress, such as shearing under load, was applied to the film. Also, Dalsin and Messersmith[20] showed that the consensus decapeptide of mfp-1 performed 10 times better than DOPA alone at anchoring PEG to TiO_2. This suggests that there is more involved in mussel adhesion than just DOPA adhesion. Nevertheless, DOPA obviously plays an important role in wet adhesion that needs to be better understood.

In this study we attempt to understand the role of DOPA in wet adhesion using a mfp inspired synthetic co-polymer of N^5-(2-hydroxyethyl)-L-glutamine and DOPA which we refer to as a mussel-inspired peptide. Using the synthetic mussel-inspired peptide allows us to control specific aspects of the peptide, such as DOPA concentration, independent of the

other factors that may be present in mfps. The adhesion mechanisms of thin films of this mussel-inspired peptide are studied on mica and TiO_2 surfaces in the SFA (Figure 1). This technique allows us to study both the adhesion of the peptide thin films to substrates as well as the cohesion between mussel-inspired peptide films under different conditions. The SFA is unique in that rather than studying individual DOPA-substrate interactions as has been done in the AFM[19,21] we observe the interaction as a function of the distance between thin films of polymer interacting over areas of 0.01 mm^2 and directly measure the adhesion energy (per unit area) of the film. Furthermore, we can observe changes in the properties of the peptide film, such as thickness, elasticity and adhesion, as a function of time, solution conditions, or loading history which give insight into the structure and behavior of the peptide films. This situation is similar to what will likely be encountered in the use of DOPA-containing polymers as biomimetic adhesives in medical and industrial applications and therefore are important properties to understand in the engineering of these adhesives.

2. Results

2.1. Adsorption of Mussel-Inspired Peptide to TiO_2

Adsorption of the mussel-inspired peptide to TiO_2 surfaces was characterized by QCM (Figure 2). A 20 μg mL^{-1} solution of peptide dissolved in acetate buffer was injected into the QCM at time $t = 0$ and allowed to adsorb to the TiO_2 surface. As peptide adsorbs, the resonant frequency of the oscillating quartz crystal decreases due to the increased mass adsorbed to the surface. Simultaneously, the QCM monitors the dissipation of the oscillations of the crystal which increase as the peptide adsorbs to the surface indicating that the adsorbed layer is soft and dissipative. At 52 min the QCM was flushed with clean acetate buffer indicated by a small spike in the frequency at this time. Flushing with buffer did not significantly change the frequency or dissipation indicating that the peptide is not easily rinsed off after adsorption has taken place. Subsequent rinses with acetate buffer yielded similar responses. The final frequency shift of 52 Hz corresponds to an adsorbed mass of 0.28 μg cm^{-2} by the Sauerbrey equation. UsingaVoigt-basedmodel[23,24] the frequency and dissipation can be used to estimate many properties of the visco-elastic film. The model gives a viscosity of the mussel-inspired film of 7.5 cP, a film thickness of 3.5 nm and shear modulus of 6×10^5 Pa. This viscosity and shear modulus are similar to those measured for an mfp-1 film after crosslinking of the DOPA residues have been induced in the film.[24] Although the mussel-inspired peptide is not crosslinked in our experiments the viscosity may be similar to mfp-1 crosslinked films due to the fact that the mussel-inspired peptide has a much smaller molecular weight (5 kDa vs. 120 kDa), lacks the decapeptide repeats of the mfp-1, and has a higher DOPA concentration and almost certainly a higher affinity for the TiO_2.

In preparing the SFA surfaces the mussel-inspired peptide was allowed to adsorb to the SFA surface for 20 min before excess was rinsed away. From Figure 2 we see that 95% of the final mass has adsorbed within 20 min and the dissipation has reached a steady state value. The SFA experiments typically measured a film thickness of 3–5 nm on TiO_2 and mica. Although the QCM is not conductive to adsorption measurements on mica, we can be certain that peptide adsorbs to form a robust film on mica due to the hard wall at 3-5 nm in the SFA experiments which does not change on repeated compressions of the film (force runs) or squeeze out under high loads (>100 MPa).

2.2. Comparison of Mussel-Inspired Peptide to Mfp-3

Lin et al.[22] measured the adhesion of mfp-1 and mfp-3 to mica surfaces in the SFA. Figure 3 shows a comparison of force runs between mfp-3 films (Figure 3a) and mussel-inspired peptide films (Figure 3b) adsorbed on mica in acetate buffer after the surfaces were left in

contact for 30 min. The mussel-inspired peptide shown in Figure 3b has a MW of 6.4 kDa and a DOPA concentration of 18 mol%, both chosen to be similar to mfp-3. It is obvious from Figure 3 that the force curves are qualitatively similar for each peptide. In both cases repulsive forces are measured upon approach beginning at a separation distance of 8–10 nm. The hard wall for the mfp-3 films is at 2 nm whereas the hard wall for the mussel-inspired peptide film is at 4 nm, which suggests that it is thicker than the mfp-3 film, likely due to differences in the deposition of the films. The mfp-3 film was deposited in situ when the opposing surfaces were separated by only a few hundred nanometers, which may have hindered the ability of the mfp-3 to diffuse to and deposit in the contact area, whereas the mussel-inspired peptide was allowed to adsorb from a droplet on the bench-top without an opposing surface, therefore allowing for a fast and complete deposition of the film. Additionally, cooperative interactions within the mfp-3 film may also contribute to the thinner films and stronger adhesion energy (also discussed below).

On separation adhesive forces are measured until the surfaces jump apart at a force of F_{ad} = 3 mN m^{-1} for the mfp-3 film. This adhesion force corresponds to an adhesion energy of $W_{ad} = F_{ad}/2\pi R$ = 0.48 mJ m^{-2} where R is the radius of curvature of the SFA surfaces (~1–2 cm; for a definition of the variables, please see the experimental section). Similarly, an adhesion force of 2.5 mN m^{-1} (W_{ad} = 0.40 mJ m^{-2}) is measured for the mussel-inspired peptide films. The distance to which the surfaces jump apart is a reflection of the spring constants used in each experiment rather than the adhesive abilities of the films. Significantly, Figure 3 shows that the majority of the adhesion strength (80%) of mfp-3 can be directly attributed to DOPA. However, the difference in the adhesion energies of mfp-3 and the mussel-inspired peptide is not insignificant. It may be attributed to a number of factors including i) different amounts of protein/peptide adsorbed to the surfaces, ii) contributions to the adhesion from non-DOPA amino acids in the mfp-3 (these could be either direct adhesive interactions with the surface or structural factors that may align or force the DOPA residues to take a more favorable conformations such as aligning them), or iii) small differences in the amount and/or oxidative state of the DOPA residues in the mfp-3 and mussel-inspired peptide. Recent studies by Yu, et al. have shown that the purification techniques and storage conditions/time of mfp-3 can significantly affect the adhesion energies of mfp-3 thin films, attributable to oxidation of catechol to quinone in the DOPA residues.

2.3. Adhesion to TiO_2 and Mica

A series of asymmetric force runs (Figure 1) were done on thin films of mussel-inspired peptides with DOPA concentrations of 0, 3, 10, and 18 mol% in order to directly measure the adhesion to mica and TiO_2. The results are shown in Figure 4 for 0, 10, and 18 mol% DOPA. The 0 mol% DOPA peptide, or poly(hydroxyethyl glutamine) (6.6 kDa), was not adhesive enough to either the mica or TiO_2 to measure an adhesion force upon separation. It does however appear to adhere weakly, at least enough for the peptide to form a layer on the surfaces which is evident by the hard walls at 5 nm on both the mica and TiO_2 (top 2 force curves in Figure 4). Regardless, this control experiment shows that the hydroxyethyl glutamine does not contribute significantly to the adhesion energies measured with the DOPA containing peptides. The force curves shown for poly(hydroxyethyl glutamine) films against mica and TiO_2 were reproducible and non-adhesive over many force runs, including long contact times and compression to high loads.

The DOPA containing mussel-inspired peptides did adhere to mica as shown in the bottom two force curves on the left side of Figure 4. For the 10 mol% DOPA peptide (7.1 kDa) the forces measured upon approach had a longer ranged repulsion than the other films on mica, probably due to a thicker peptide film on this particular deposition. The repulsive force measured on approach was reproducible and consistent for multiple approaches. We interpret this as weakly adhering peptides to the base layer which were not rinsed away prior

to the experiment. Note that the hard wall at 5 nm is consistent with the hard walls of the other films. Adhesion was measured upon separation, culminating in a jump out at a force of F_{ad}/R = 0.2 mN m^{-1} and a distance of D = 15 nm. The adhesion energy in this case is interpreted as the difference between the force on approach and separation at 15 nm, W_{ad} = 0.05 mJ m^{-2}. The 18 mol% DOPA peptide had a very sharp hard wall at 5 nm and an adhesion energy of W_{ad} = 0.2 mJ m^{-2} on mica. The force curves did not depend on load or contact time between the mica and peptide films.

The DOPA containing mussel-inspired peptide adheres much more strongly to TiO_2 (right side of Figure 4) than to mica. Additionally, the adhesive strength of the films increased if the film was left in contact with the TiO_2 for long times (1 h). For 10 mol% DOPA peptide the adhesion measured during a typical force run when the surfaces are left in contact for min yields an adhesion energy of W_{ad} = 0.26 mJ m^{-2} on TiO_2,about 4–5 times stronger than on mica. However, if the surfaces are left in contact for h the adhesion energy increases to W_{ad} = 0.6 mJ m^{-2}, about twice that of the 1 min contact time to TiO_2 and an order of magnitude larger than the adhesion to mica. Similarly, at a DOPA concentration of 18 mol% the mussel-inspired peptide adheres to TiO_2 with an adhesion energy of W_{ad} = 0.5 mJ m^{-2} for contact times of 1 min, but increases to W_{ad} = 0.86 mJ m^{-2} for contact times of 1 h. Additionally, after being left in contact for an hour the film thickness appears to have decreased from 9 nm to 6 nm, which was not observed with the 10 mol% DOPA film. Upon separation the film expands but the force curve appears to go through a linear region from a distance of 7.5 to 13 nm before jumping out (the linear region is also present in the 10 mol% DOPA peptide curve but is less obvious). The force run immediately following this does not appear any differently than previous force runs on approach or separation, meaning that the thinning in the film is not a permanent change in the morphology of the film, but rather a load and time induced change in the film that couples with an increase in the adhesion (see discussion below). If left in contact for 10 min (data not shown) the film appears to thin slightly, but upon separation the adhesion does not change significantly from the 1 min contact time. Also, note that at DOPA concentrations of 18 mol% the adhesion was strong enough to observe a jump into contact from 30 nm. Interestingly, for the 1 min contact times the jump out occurred at 17 nm, the same distance that the surfaces jumped in to. However, after 1 h contact time the jump out occurred at a distance of 14 nm, a difference of 3 nm from the 1 min contact time and consistent with the shift in the hard wall due to the thinning of the film. The jump in was not observed at lower DOPA concentrations or on mica, likely due to weaker adhesion energies. Figure 5 shows a summary of the adhesion energies of the mussel-inspired peptide films to mica and TiO_2 as a function of DOPA concentration. The adhesion to mica (squares) is 0.09 μJ m^{-2} mol^{-1} and was not affected by long contact times. Adhesion to TiO_2 is 0.29 μJ m^{-2} mol^{-1} for short contact times (circles) and increases to 0.51 μJ m^{-2} mol^{-1} for h contact times (triangles). The reason for the increase in the adhesion to TiO_2 after long contact times is likely due to rearrangements of the DOPA residues within the film. Initially the DOPA residues will likely be oriented randomly (or perhaps a higher percentage adhered to the underlying TiO_2 substrate) and when the film is brought into contact with an opposing TiO_2 surface the DOPA readily available at the surface of the film will adhere. This adhesion energy is likely what is being measured for the short contact times of min. However, if the film is left in contact with the opposing TiO_2 surface long enough it is reasonable to believe that if the DOPA-TiO_2 interaction is strong the DOPA residues that may have originally been in the interior of the film will work their way to the TiO_2 surface and increase the adhesion energy of the film. This mechanism is not observed on mica, probably due to the relatively weak interaction between DOPA and mica which is fairly inert.

2.4. Stress-Induced Phase Transition on TiO_2 Surfaces

An interesting feature in the force curves on TiO_2 for the mussel-inspired peptide films with 18 mol% and 10 mol% DOPA is the appearance of a linear region in the separation force curve just before the surfaces jump apart. The linear region only appears after the surfaces have been left in contact for 60 min, is accompanied by an increase in adhesion (discussed above), and is most easily observed in the 18 mol% DOPA peptide film. As the surfaces are separated the force decreases as the spring load is relaxed, becoming attractive as normal. However, the force curve becomes linear from about 7 to 13 nm just before the surfaces jump apart. Similarly, the 10 mol% DOPA peptide film has a linear region between 12 and 18 nm upon separation, although somewhat less obvious. These are in stark contrast to the smooth curves observed in the short contact time (1 min) force runs on TiO_2, or any of the force runs done with DOPA concentrations below 10 mol% on TiO_2 or on any of the force runs on mica surfaces.

As previously mentioned, the force between two curved surfaces is proportional to the energy between flat surfaces, $W = F/2\pi R$. The energy between flat surfaces is related to the pressure by $P = -\mathrm{d}W/\mathrm{d}D$, and hence the derivative of the force curves plotted in Figure 4 yields the pressure as a function of distance. Figure 6 shows the pressure P within the mussel-inspired peptide films during the decompression (separation) and adhesion of the film after high contact times to TiO_2. The inset shows the original separation force curves with the differentiated data highlighted in the grey box. The pressure-distance curve clearly shows a constant region at 50 kPa for mussel-inspired peptide films with 18 mol% DOPA and 15 kPa for the films with 10 mol% DOPA, which indicates a first order phase transition in the peptide film.

One possible reason for this behavior is π–π stacking of the aromatic rings in the DOPA residues. This mechanism would explain why the phase transition is DOPA-dependent and requires time in contact for the DOPA residues to rearrange. Furthermore, this could explain why the 18 mol% DOPA mussel-inspired peptide film appears to thin after the surfaces are left in contact for 1 h. Although thinning is not observed in the 10 mol% DOPA film, this could be due to the lower DOPA concentration, and hence less thinning would be expected upon π–π stacking that may not have been detected in the SFA experiment. Rearrangement of DOPA within the films is also consistent with the explanation used to justify the increase in adhesion to TiO_2 with contact time. That is to say, the phase transition to another conformation should improve adhesion if it effectively repositioned more DOPA residues onto one or both interfaces. It is hard to imagine how this could happen in a random copolymer, but sequences with synthetic DOPA peptides are rarely random.

Phase transitions in similar polymers and peptides have been observed previously. For example, it is known that poly(hydroxyethyl glutamine) is randomly coiled in water, but is α-helical in aqueous methanol.[25] However, it is unlikely that hydroxyethyl glutamine is responsible for the phase transition observed here which is more prevalent at higher DOPA concentrations and hence lower hydroxyethyl glutamine concentrations. Mfp-1 has also been shown to undergo osmotic pressure induced conformational changes in solution which may be a way for the mussel to control the reactivity of the mica.[26] Also, under physiological conditions mfp-1 is known to contain helix-like or turned deca-peptide segments[27] that may accommodate conformational changes. However, these structures are not present in the mussel-inspired peptides studied here.

Phase transitions of this kind have not yet been observed in mfp films, however, if present would give the mussel a few obvious advantages. An adhesive that is compliant over a given distance at a given pressure, such as the 18 mol% DOPA peptide film studied here, has a much higher toughness (integrated adhesion energy) than a rigid adhesive. Also, 50 kPa, the

pressure at which the phase transition takes place, would give rise to an adhesive strength of 0.5 N (or 50 g) for a typical mussel plaque with an area of 10 mm^2. This is on the same order of the forces a mussel would likely experience if attached to a rock in nature. Combined, these two properties would give the mussel an adhesive with a high toughness at physically relevant pressures and enhance its chance of staying attached to rocks for long periods of time.

2.5. Oxidation of DOPA

The oxidation state of DOPA has been known to affect the adhesion[19] as well as crosslinking within mfp networks[1,5,17] and so the effect of oxidation on the cohesion of two mussel-inspired peptide films is of interest. To study the effect of oxidation on DOPA adhesion, SFA experiments with a symmetric geometry were performed in which mussel-inspired peptide films with a DOPA concentration of 27 mol% (6.3 kDa) were deposited on opposing mica surfaces (Figure 7). In the experiment the measured adhesion forces are the result of cohesion between the peptide films rather than adhesion to mica. Figure 7 a shows the interaction between mussel-inspired peptide films with DOPA residues in their reduced state (structure shown in the inset). The force curves look similar to those observed in the asymmetric experiments on mica in Figure 4 with a weak, short ranged repulsion on approach and a hard wall at a distance of 7 nm (i.e., each film has a thickness of 3.5 nm) followed by adhesion and a jump out on separation. The cohesion strength between the films is measured to be 2.1 mN m^{-1} (0.33 mJ m^{-2}).

Figure 7b shows the effect of adding sodium periodate ($NaIO_4$) to the buffer solution between the mussel-inspired peptide films. Periodate is a strong oxidizing agent and was added to the droplet between the surfaces at a concentration of 0.5 mM, well in excess of the estimated DOPA available for oxidation. Periodate is known to oxidize catechol to quinone,[28,29] and hence convert the DOPA residues in the peptide to the quinone form shown in the inset of Figure 7b. The addition of periodate appears to have a two-fold effect on the force profile of the films. The first is that the adhesion is significantly reduced to the point that it is no longer measurable in the SFA. This can only be due to the oxidation of the DOPA and emphasizes that quinone does not adhere as strongly as DOPA.[30] This result has significant implications to the preparation and storage conditions of DOPA containing adhesives as any amount of oxidation dramatically reduces the effectiveness of the adhesive.

The second effect of adding periodate is that the film thickness appears to increase significantly. On approach, repulsive forces begin to appear at distances of 25 nm and the hard wall is reached at 10 nm. This effect could be due to peptide crosslinking between the DOPA residues within the films which has been reported before for other DOPA containing polymers[5] as well as mfps.[17,31,32] Although it is not obvious that crosslinking should make the film thicker, in fact others have reported that crosslinking within mfp-1 caused the film to get thinner,[24] one possible explanation is that the crosslinking between adjacent mussel-inspired peptides adsorbed on the surface causes the peptides to form larger agglomerates of multiple peptides that protrude away from the surfaces and simultaneously reduce the coverage of the film on the mica surface. This would also be consistent with the reduced adhesion of the DOPAquinone residues to the mica. In this explanation, the film essentially acts like a rough surface with patches that protrude out causing long-range repulsion forces on compression and decompression.

An alternative explanation for the long-range repulsive forces measured after oxidation is tautomerization of the DOPAquinone, resulting in migration of the double bond to the peptide backbone and reduction of the quinone to α, β-dehydroDOPA, followed by subsequent formation of α, β-dehydroDOPAquinone. This chemistry is well known for quinones[33,34] and, given that the α-carbon is in the peptide backbone would result in a

significantly more rigid polymer. The rigidity of the polymer, along with reduced adhesion due to DOPA oxidation, could lead to rougher films and longer range repulsive forces as packing would be less favorable.

Although periodate is known to oxidize catechol to quinone, the pH is also known to be an important factor in the oxidative state of DOPA.[5] At pH 5.5 DOPA is in its reduced state and is capable of the strong adhesive interactions discussed above. However, Figure 8 a–b show the effect of increasing the pH from 5.5 to 7.5 on the interaction between mussel-inspired peptide films. At pH 7.5 the adhesion is negligible, similar to the effect of adding periodate. However, unlike adding periodate the oxidation caused by increasing the pH does not induce long ranged repulsive forces and hence does not appear to have as drastic of an effect on crosslinking or tautomerization of the DOPA residues within the film. Upon increasing the pH to 7.5 (Figure 8b) the repulsive forces do extend further than at pH 5.5 (Figure 8a), indicating some amount of crosslinking may have occurred, but the forces are much smaller than observed after adding periodate (Figure 7b).

Interestingly the effect is not reversible, i.e., going from pH 7.5 to pH 5.5 does not restore adhesion (within h) to the peptide films. Whereas reduction of the quinone to DOPA may occur over time at pH 5.5, we did not detect evidence for it within the time frame of the experiments performed here. However, the addition of a thiol containing polymer did restore some adhesion (Figure 8). The thiol-containing polymer was selected due to reported crosslinking ability,[8,12] but it appears the recovery of some adhesion might actually be due to the reducing effect of thiols on the DOPA as illustrated in the inset of Figure 8c. This is actually the more likely scenario as the thiol-catechol adduct has a lower redox potential than the catechol and would not be an effective reduction. Regardless of the mechanism, the adhesion is restored (F_{ad}/R = 0.75 mN m^{-1}, Figure 8c), though not completely to the level of the pre-oxidized state (F_{ad}/R = 2.2 mN m^{-1},Figure 8a).

3. Discussion

3.1. Estimating the Strength of the DOPA-Mica and DOPA-TiO_2 Interactions

The strength of the DOPA-TiO_2 interaction has recently come under some scrutiny as conflicting reports measured the interaction strength between 600–900 pN[19] and 67 pN[21] per bond by AFM. Assuming a bond length of a hydrogen bond, 0.2 nm, this puts the reported value of the DOPA-TiO_2 bond energy at anywhere from 8 to 110 kJ mol^{-1}. For comparison the energy of a hydrogen bond is in the range of 10-30 kJ mol^{-1}. Using the QCM adsorption data and the SFA adhesion force measurements we can estimate the strength of the DOPA-TiO_2 and DOPA-mica interactions. Assuming the mussel-inspired peptide adsorbs at the same rate to the SFA surfaces as it does to the QCM surfaces (there is no reason to believe differently), the density of mussel-inspired peptide on a TiO_2 surface after 20 min (the time allotted for adsorption to SFA surfaces) is about 95% of the final mass adsorbed in the QCM experiment, or 0.26 μg cm^{-2}. The adhesion energy (after 60 minute contact times) measured for the peptide film with 18 mol% DOPA to TiO_2 is W_{ad} = 0.86 mJ m^2. In order to estimate the energy per DOPA-TiO_2 bond we must know how much DOPA is adsorbed to each of the TiO_2 surfaces in the SFA experiment. Unfortunately this is unknown but using 50% at each interface, the maximum amount of DOPA residues in direct adhesive contact with the TiO_2 surface possible, will give a lower bound for the strength of the DOPA-TiO_2 interaction. Doing this gives 0.64 kJ mol^{-1} for a lower bound estimate of the DOPA-TiO_2 adhesion that turns out to be an order of magnitude lower than the lower end of reported values measured by AFM. Although 50% of the DOPA residues are not likely to be attached to each surface in the SFA experiments, in order to arrive at the lower end of the reported adhesion energies would require 5% of the DOPA residues in the mussel-inspired peptide film to be adhering to the opposite TiO_2 surface, well within the

range of feasible values. Note that the strength of the DOPA-TiO_2 complexation is known to increase with pH, which is something that needs further scrutiny in the future.

For completion we can do the same calculation for the DOPA-mica interaction using an adhesion energy of W_{ad} = 0.2 mJ m^{-2} for the 18 mol% DOPA peptide. This calculation has the added inaccuracy that we must assume the density of mussel-inspired peptide on mica is the same as that on TiO_2. Nevertheless, the analysis gives an energy per DOPA-mica bond of 0.15 kJ mol^{-1} as a lower bound estimate. Note that the SFA measurements showed that the DOPA residues are much more likely to rearrange into an optimal configuration for adhesion on TiO_2 than on mica, and hence the lower bound calculated for the DOPA-TiO_2 interaction is likely to be much closer to the true value of the bond than the DOPA-mica calculation.

3.2. Adhesion Mechanism to Mica and TiO_2

The adhesion of the mussel-inspired peptides, and by extension DOPA, to TiO_2 is much stronger than to that of mica. Although the exact mechanism of the interactions between DOPA and TiO_2 or mica cannot be determined from these results, a probable mechanism can be speculated, and illustrated in Figure 9. Martin et al.[18] have shown that catechol forms bidentate binuclear surface complexes on TiO_2 particles (each OH group from the catechol binds to a separate Ti molecule on the exposed surface) in solution that appear to have a 40% covalent and 60% ionic bond characteristic. These coordination complexes are known to form between catechol and other metal oxides such as Ti IV and Fe III[19,20] as well as oxide surfaces such as alumina[30] and are almost certainly responsible for the abnormally strong interaction between DOPA and TiO_2.

The adhesion mechanism of DOPA to mica is much weaker and likely not due to a specific coordination complex as it is with TiO_2. Lin et al.[22] point out that the adhesion of mfp-3 to mica is actually relatively weak but that the geometry of the plaque as well as the presence of multiple plaques at different angles are more than adequate to hold a mussel firmly in place. Furthermore, mica is known to be chemically very inert and undergoes no known chemical reactions. A freshly cleaved mica surface exposes Si, O, and some K^+ atoms[35] depending on the pH and ionic conditions of the solution. Although speculation, the DOPA-mica interaction may be due to hydrogen bonding between the OH groups of the catechol and the O atoms in the mica crystal as illustrated in Figure 9. Interestingly, the distance between adjacent O atoms in the mica crystal is 0.28 nm apart[35] and the distance between OH groups in DOPA are 0.29 nm apart. However, these hydrogen bonds will still have to compete with water molecules at the interface and hence the resulting interaction is rather weak.

4. Experimental Section

Peptide Synthesis and Characterization:

The mfp inspired peptide used in these experiments was a random co-polymer of 3,4-dihydroxyphenyl-L-alanine (DOPA) and N^5-(2-hydroxyethyl)-L-glutamine (Figure 1). Hydroxyethyl glutamine was chosen to enhance solubility of the peptide (polyDOPA is not soluble in water) and because it is not expected to contribute to the adhesion of the peptide, thus enabling a focus on the adhesion characteristics of DOPA.

α-Amino acid *N*-carboxyanhydrides (NCAs) of O,O'-diacetyl DOPA and γ-benzyl glutamic acid (Sigma-Aldrich) were synthesized by phosgenation according to the procedure described by Fuller et al.[36] NCAs were thoroughly purified by multiple crystallizations and immediately stored inside an Ar-filled glove box. Peptide copolymers were synthesized by ring opening polymerizations of NCA using hexamethyldisilazane (HMDS, Sterm

Chemicals) as initiators.[37] Removal of the acetyl and benzyl protecting groups was effected by aminolysis with 2-aminoethanol (Fluka) following previously described literature procedures.[36,38] All polymers were purified by multiple precipitation and centrifugation cycles followed by extensive dialysis against nanopure water. They were subsequently lyophilized and stored at − 80 ° C. The hydroxyethyl glutamine homopolymer was synthesized in the same manner, with the exclusion of the DOPA NCA. A representative procedure for the synthesis of the copolymer is provided in supporting material as well as a reference for full details.

Modification of the monomer feed resulted in polymers with DOPA concentrations of 0, 3, 10, 18, and 27 mol% with molecular weights in the range of 5.9–7.1 kDa (polydispersity index or PDI < 1.1) as measured by gel permeation chromatography (GPC) using a Waters 2690 separation module equipped with a waters 2414 differential refractometer and Waters 2998 Photodiode Array Detector (PDA) (Waters Corp., Mildford, MA). Separation was effected on Viscotek I-MBHMW-3078, I-Series mixed bed high molecular weight and I-Series mixed bed low molecular weight columns (separation range 100 ~ 20 k) using dimethylformamide (DMF)/0.01% LiBr as solvent. The narrow PDIs are a result of using HMDS as an initiator, as recently reported by Lu and Cheng,[37] which leads to polymers with predicted MWs and narrow MW distributions. The DOPA:hydroxyethyl glutamine ratios were then verified by NMR recorded on a Bruker Avance DMX 500 MHz spectrometer. Polymers were stored in a dessicator for up to 4 months until ready for use.

The thiol polymer was a random co-polymer of *α*,*β*-(2-hydroxyethyl)-$_{DL}$-aspartamide and *α*,*β*-(2-mercaptoethyl)-$_{DL}$-aspartamide synthesized by the thermal polymerization of aspartic acid[39] with subsequent treatment with 2-aminoethanethiol and 2-aminoethanol. The resulting co-polymer had a molecular weight of 30 kDa (PDI = 1.6) with a thiol concentration of 15 mol%.

SFA Experiments:

Prior to experiments the polymers were dissolved in 10 m$_M$ acetic acid (Sigma-Aldrich), 250 m$_M$ KNO_3 (Sigma-Aldrich), pH 5.5 buffer solution at a concentration of 20 μg mL^{-1}. The high salt concentration provides a similar saline level as in seawater. Sodium periodate, $NaIO_4$, (Sigma-Aldrich) was prepared prior to each experiment at a concentration of 1 m$_M$. Milli-Q water (Millipore) was used for all cleaning and solution preparation.

The force between the mussel-inspired peptide thin films was measured in an SFA 2000 which has been described in detail elsewhere.[40,41] Briefly, the technique directly measures the force *F*, attractive or repulsive, between surfaces with a crossed-cylinder geometry (locally identical to a sphere-sphere or sphere-flat geometry) as a function of the distance *D* between the surfaces. Mica SFA surfaces are made with freshly cleaved, uniformly thick muscovite mica sheets approximately 2 cm^2, back-silvered with 55 nm of silver, then glued onto cylindrical silica disks with a radius of curvature *R* ~ 2 cm. TiO_2 surfaces were made by depositing 10 nm of TiO_2 onto the mica discs by E-beam deposition (Temescal system) at a rate of 0.1 nm s^{-1} and a pressure < 4 × 10^{-6} Torr. The TiO_2 films had a roughness of ~ 1 nm measured by AFM (Veeco Dimension 3100, Veeco Instruments) and were shown to be free of impurities by XPS (Kratos Ultra, Kratos Analytical Limited). The distance between the surfaces *D* is measured with an optical technique based on multiple beam interference fringes (fringes of equal chromatic order, FECO) where *D* is determined with a resolution of ±1Å from measurements of the wavelength of the FECO fringes in a spectrometer. The distance between the surfaces is controlled with a series of coarse and fine micrometers and piezoelectric crystals. The force between the surfaces is determined by the deflection of a double cantilever spring of stiffness *K* supporting the lower surface. Due to differences in the radius of the surfaces *R* from the gluing process it is customary to normalize the force *F*

by R when comparing SFA measurements. The normalized force F/R between the two cylindrical SFA surfaces is directly proportional to the energy between two flat surfaces by the Derjaguin approximation,[42] $E(D) = F(D)/2\pi R$. Throughout this paper the distance $D = 0$ will refer to the distance measured at flat contact of the surfaces (either mica or TiO_2) prior to depositing the peptide thin films.

Mussel-inspired peptide films were made by adsorbing polymer from a 20 μg mL^{-1} solution onto the SFA discs for 20 min, then rinsing the excess polymer away with clean acetate buffer. During the polymer adsorption the discs were kept in a closed Petri dish to control for evaporation. The discs were then mounted in the SFA in one of two configurations. In an asymmetric configuration the mussel-inspired peptide was adsorbed on one surface whereas the opposite surface was left clean in order to measure the *adhesion* between the film with mica and TiO_2. A schematic of the SFA surfaces in an asymmetric configuration with TiO_2 surfaces is shown in Figure 1. In a symmetric configuration the mussel-inspired peptide film was deposited on both surfaces in order to measure *cohesion* between the films. The mussel-inspired peptide films were always hydrated (i.e., never allowed to dry) and a droplet of clean acetate buffer was injected between the surfaces immediately after loading in the SFA. Hydration is visually monitored throughout the experiment with the fringes and directly through an eyepiece on the microscope focused on the contact region. The surfaces are mounted in a sealed container in the SFA, which minimized evaporation of the droplet, which is sufficient to keep the surfaces hydrated for up to one day. All forces were measured in the acetate buffer.

QCM Adsorption Experiments:

Quartz crystal microbalance (QCM) experiments were done with a Q-Sense QCM-D300 to characterize the adsorption of the mussel-inspired peptide to TiO_2 surfaces independently of the SFA experiments. TiO_2 QCM crystals were used as purchased from Q-Sense. Prior to experiments the QCM crystals were cleaned in 3% SDS solution, thoroughly rinsed in distilled water, cleaned with ethanol and then cleaned by UV-Ozone for 10 min. Frequency and dissipation baselines were established in clean acetate buffer solution followed by injection of 20 μg mL^{-1} mussel-inspired peptide solution which began the adsorption experiment.

Supplementary Material

Refer to Web version on PubMed Central for supplementary material.

Acknowledgments

This work was funded by NIH grant #R01 DE018468.

References

[1]. Waite JH. Int. J. Adhesion Adhesives. 1987; 7:9.

[2]. Waite JH. Integrative Comparative Biol. 2002; 42:1172.

[3]. Wiegemann M. Aquatic Sci. 2005; 67:166.

[4]. Dalsin JL, Hu BH, Lee BP, Messersmith PB. J. Am. Chem. Soc. 2003; 125:4253. [PubMed: 12670247]

[5]. Shao H, Stewart RJ. Adv. Mater. 2010; 22:729. [PubMed: 20217779]

[6]. Lee H, Lee BP, Messersmith PB. Nature. 2007; 448:338. [PubMed: 17637666]

[7]. Zhao H, Robertson NB, Jewhurst SA, Waite JH. J. Biol. Chem. 2006; 281:11090. [PubMed: 16495227]

[8]. Zhao H, Waite JH. J. Biol. Chem. 2006; 281:26150. [PubMed: 16844688]

[9]. Waite JH, Qin XX. Biochemistry. 2001; 40:2887. [PubMed: 11258900]
[10]. Proudfoot GM, Ritchie IM. Aus. J. Chem. 1983; 36:885.
[11]. Sternson LA, Sternson AW. Chem.-Biol. Interact. 1973; 7:143. [PubMed: 4768575]
[12]. Zhao H, Waite JH. Biochemistry. 2005; 44:15915. [PubMed: 16313194]
[13]. McDowell LM, Burzio LA, Waite JH, Schaefer J. J. Biol. Chem. 1999; 274:20293. [PubMed: 10400649]
[14]. Taylor SW, Luther GW, Waite JH. Inorg. Chem. 1994; 33:5819.
[15]. Taylor SW, Chase DB, Emptage MH, Nelson MJ, Waite JH. Inorg. Chem. 1996; 35:7572.
[16]. Sever MJ, Weisser JT, Monahan J, Srinivasan S, Wilker JJ. Angew. Chem. Int. Ed. 2004; 43:448.
[17]. Monahan J, Wilker JJ. Langmuir. 2004; 20:3724. [PubMed: 15875406]
[18]. Martin ST, Kesselman JM, Park DS, Lewis NS, Hoffmann MR. Environ. Sci. Technol. 1996; 30:2535.
[19]. Lee H, Scherer NF, Messersmith PB. Proc. Natl. Acad. Sci. USA. 2006; 103:12999. [PubMed: 16920796]
[20]. Dalsin JL, Lin LJ, Tosatti S, Voros J, Textor M, Messersmith PB. Langmuir. 2005; 21:640. [PubMed: 15641834]
[21]. Wang JJ, Tahir MN, Kappl M, Tremel W, Metz N, Barz M, Theato P, Butt HJ. Adv. Mater. 2008; 20:3872.
[22]. Lin Q, Gourdon D, Sun CJ, Holten-Andersen N, Anderson TH, Waite JH, Israelachvili JN. Proc. Natl. Acad. Sci. USA. 2007; 104:3782. [PubMed: 17360430]
[23]. Voinova MV, Rodahl M, Jonson M, Kasemo B. Phys. Scr. 1999; 59:391.
[24]. Hook F, Kasemo B, Nylander T, Fant C, Sott K, Elwing H. Anal. Chem. 2001; 73:5796. [PubMed: 11791547]
[25]. Adler AJ, Hoving R, Potter J, Wells M, Fasman GD. J. Am. Chem. Soc. 1968; 90:4736. [PubMed: 5661143]
[26]. Van Der Leeden MC. Langmuir. 2005; 21:11373. [PubMed: 16285813]
[27]. Haemers S, Van Der Leeden MC, Frens G. Biomaterials. 2005; 26:1231. [PubMed: 15475052]
[28]. Yu ME, Hwang JY, Deming TJ. J. Am. Chem. Soc. 1999; 121:5825.
[29]. Liu B, Burdine L, Kodadek T. J. Am. Chem. Soc. 2006; 128:15228. [PubMed: 17117875]
[30]. McBride MB, Wesselink LG. Environ. Sci. Technol. 1988; 22:703.
[31]. Burzio LA, Waite JH. Biochemistry. 2000; 39:11147. [PubMed: 10998254]
[32]. Haemers S, Koper GJM, Frens G. Biomacromolecules. 2003; 4:632. [PubMed: 12741779]
[33]. Rzepecki LM, Nagafuchi T, Waite JH. Arch. Biochem. Biophys. 1991; 285:17. [PubMed: 1846730]
[34]. Rzepecki LM, Waite JH. Arch. Biochem. Biophys. 1991; 285:27. [PubMed: 1899328]
[35]. Fukuma T, Ueda Y, Yoshioka S, Asakawa H. Phys. Rev. Lett. 2010:104.
[36]. Fuller WD, Verlander MS, Goodman M. Biopolymers. 1978; 17:2939.
[37]. Lu H, Cheng JJ. J. Am. Chem. Soc. 2007; 129:14114. [PubMed: 17963385]
[38]. Fuller WD, Verlander MS, Goodman M. Biopolymers. 1976; 15:1869. [PubMed: 963268]
[39]. Neri P, Antoni G, Benvenut F, Cocola F, Gazzei G. J. Med. Chem. 1973; 16:893. [PubMed: 4745831]
[40]. Israelachvili JN, Adams GE. J. Chem. Soc.-Faraday Trans. I. 1978; 74:975.
[41]. Israelachvili J, Min Y, Akbulut M, Alig A, Carver G, Greene W, Kristiansen K, Meyer E, Pesika N, Rosenberg K, Zeng H. Rep. Prog. Phys. 2010:73.
[42]. Israelachvili, JN. Intermolecular and Suface Forces. Academic Press; London: 1992.

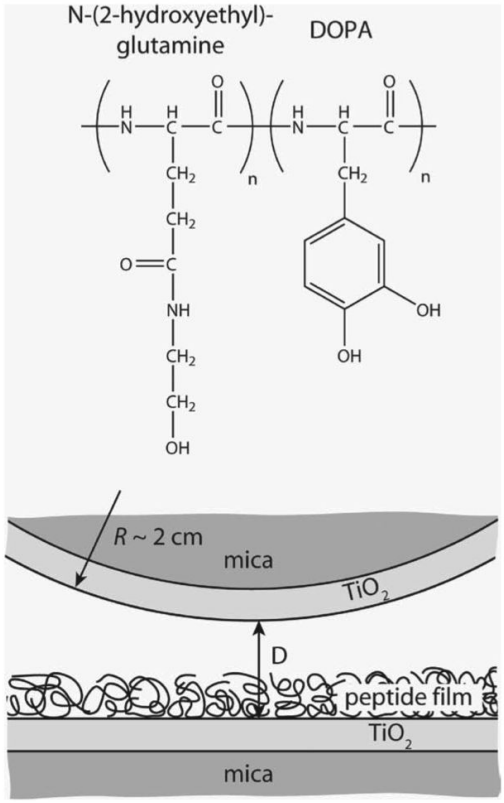

Figure 1.
The mussel-inspired DOPA-containing random copolymer used in these studies (top). Schematic of the surfaces in the SFA experiments in an asymmetric configuration used to measure the adhesion of the mussel-inspired peptide to TiO_2 (bottom).

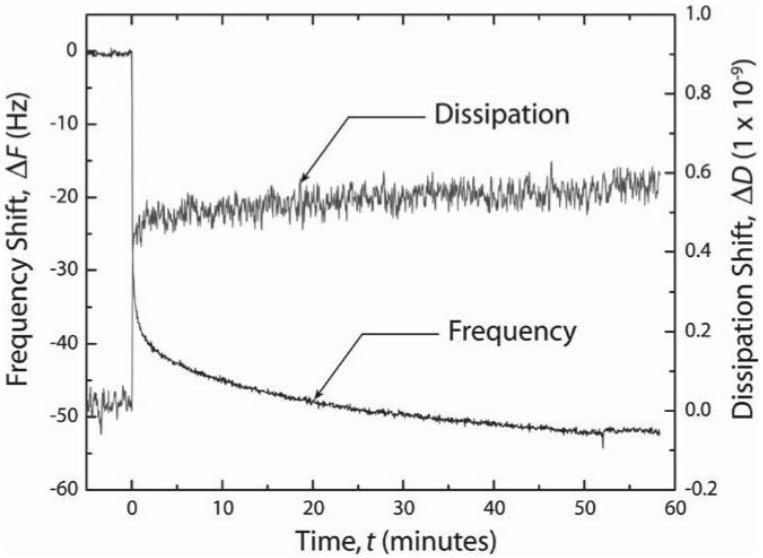

Figure 2.

QCM measurement of the frequency and dissipation shift during the adsorption of a 20 μg mL^{-1} solution of 18 mol% DOPA mussel-inspired peptide to TiO_2. The final frequency shift of 52 Hz corresponds to an adsorbed mass of 0.28 μg cm^{-2}. Within 20 min 95% of the final mass has adsorbed.

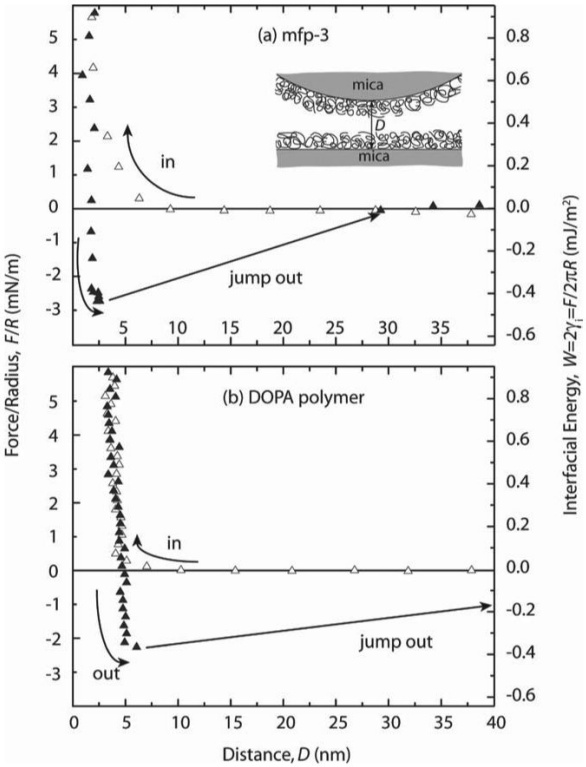

Figure 3.

Representative force runs comparing the interactions between thin films of a) mfp-3 and b) 18 mol% DOPA mussel-inspired peptide measured in the SFA. The mussel-inspired peptide is similar to mfp-3 in DOPA concentration and molecular weight. In each case the surfaces were left in contact for >30 min before separating. Mfp-3 data is reproduced from Lin et al.[22]

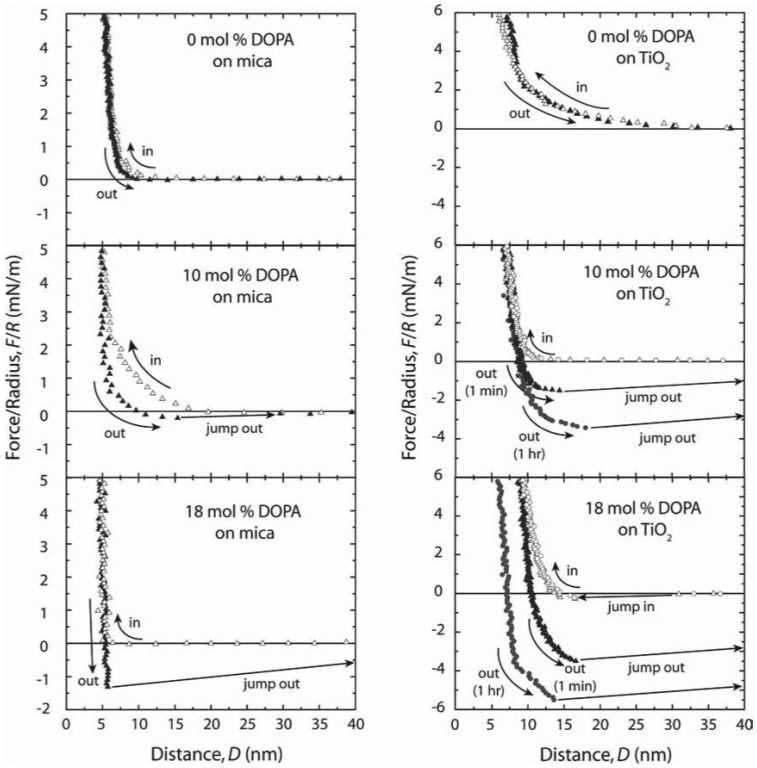

Figure 4.

Representative force runs showing the adhesion of mussel-inspired peptide to mica left) and TiO_2 (right) with increasing DOPA concentration and contact times as indicated in each force curve.

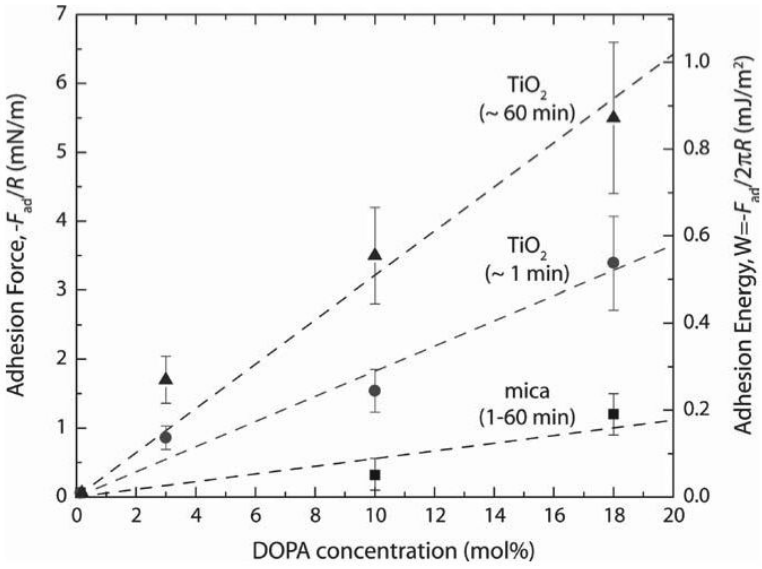

Figure 5.

Summary of the adhesion energy of the peptide films to TiO_2 and mica as a function of concentration. Adhesion to mica is not affected by contact time, but adhesion to TiO_2 increases with contact time. Error bars are one standard deviation of 6–10 measurements for the mica and TiO_2 (1 min). Due to time constraints during each experiment there were not enough data points for the TiO_2 (60 min) for a valid statistical analysis and so the error bars shown are ±20%, which was the largest error found in any of the other measurements.

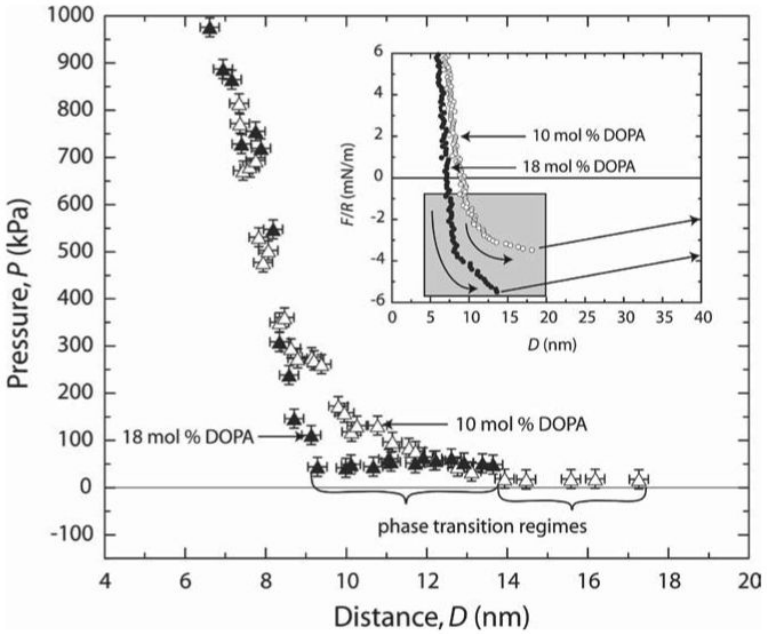

Figure 6.

Pressure ($P = -dW/dD$) vs. distance for the separation of 18 and 10 mol% DOPA mussel-inspired peptide on TiO_2 after a contact time of 1 h. The region of constant pressure at 50 kPa for 18 mol% DOPA peptide and 15 kPa for 10 mol% DOPA peptide are characteristic of a phase transition. Inset) The original separation force-distance profiles. The pressure-distance curves were generated by differentiating the data in the grey box.

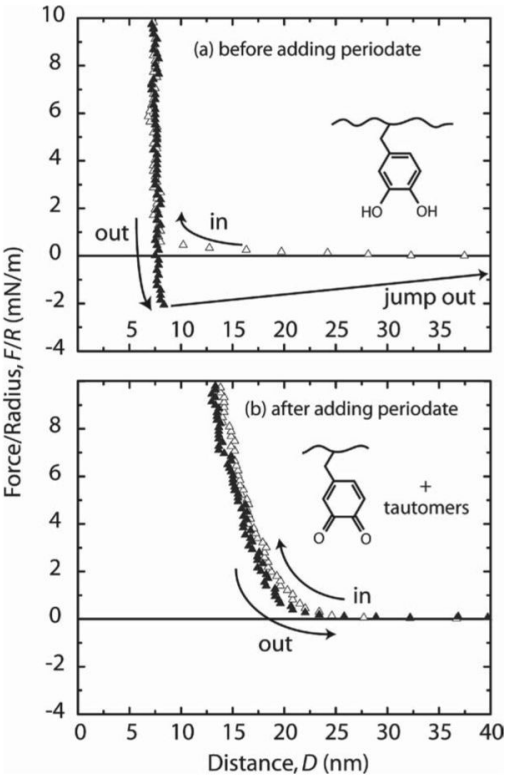

Figure 7.

Representative force runs showing the interaction between 27 mol% DOPA mussel-inspired peptide films at pH 5.5 a) before and b) after adding the oxidizing agent periodate. Insets show the oxidative state of the DOPA residues.

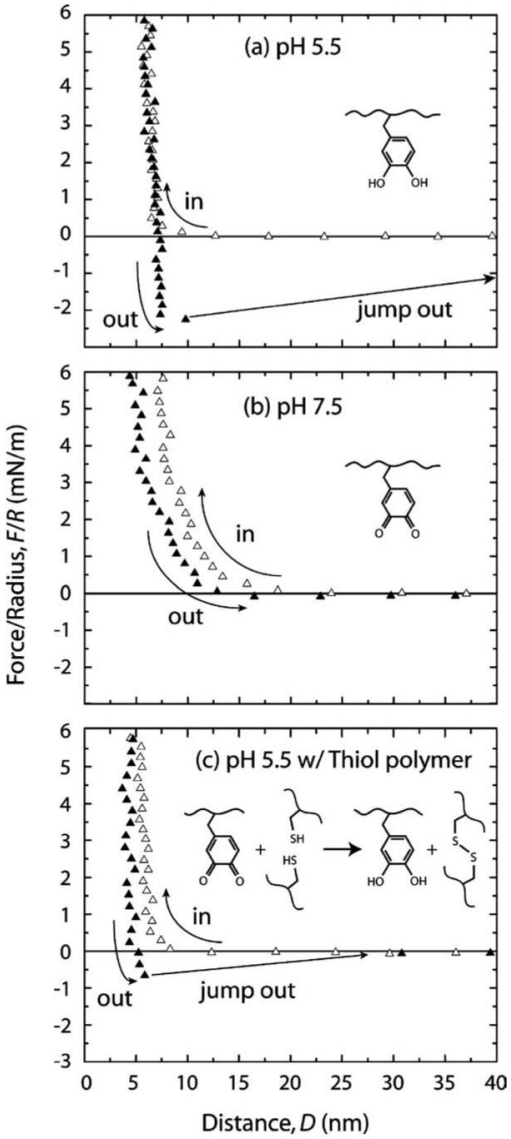

Figure 8.

The interaction between 27 mol% DOPA mussel-inspired peptide films as a function of pH. Top: Representative force run at pH 5.5 with freshly deposited mussel-inspired peptide showing strong adhesion. Middle: Representative force run between the same peptide films after increasing the pH to 7.5. Bottom: Representative force run between the same peptide films after reducing the pH back to 5.5 and adding a thiol containing polymer. Adhesion has been restored but with lower adhesion strength than originally measured. Insets show possible interactions responsible for the adhesive behavior of the DOPA.

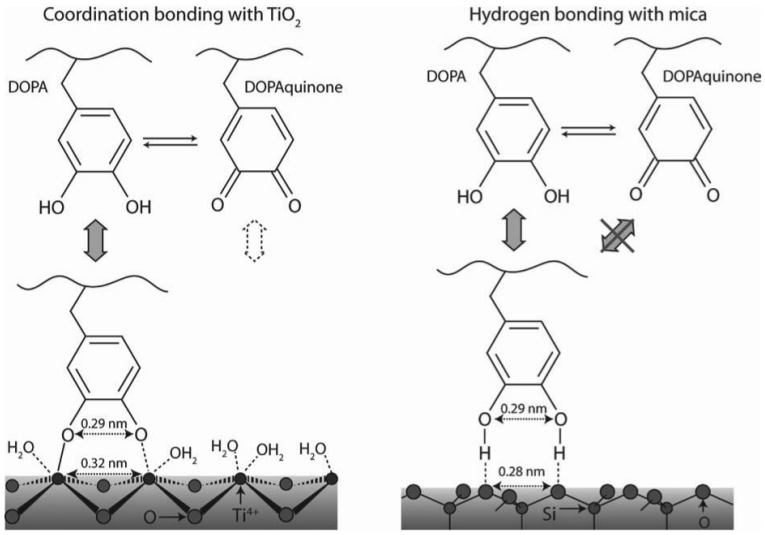

Figure 9.

Illustration of the proposed binding mechanism of DOPA to TiO_2 and mica surfaces. DOPA and DOPAquinone, to a lesser extent, can form bidentate binuclear complexes with the TiO_2 surface (left). In contrast, on mica (right) the interaction with DOPA is much less specific and may result from the hydrogen bonding of the phenolic OH groups to the oxygen atoms of the cleaved mica surface. DOPAquinone has no H to donate.